Sensors & Transducers, Vol. 183, Issue 12, December 2014, pp. 123-128

Sensors & Transducers

The Dynamics of Spontaneous Capillary Flow in Confined and Open Microchannels

*** Jean BERTHIER, David GOSSELIN, Noémie VILLARD, Catherine PUDDA, François BOIZOT, Guillaume COSTA, Guillaume DELAPIERRE**

CEA/Université Grenoble-Alpes, 17, avenue des Martyrs, 38054 Grenoble, France
Tel.: 0033 438783551
* E-mail: jean.berthier@cea.fr

Received: 16 September 2014 /Accepted: 28 November 2014 /Published: 31 December 2014

Abstract: Capillary microfluidics or capillarics is gaining importance in the biotechnological domain. It combines the advantages of capillary actuation that does not require pumps or syringes to move the fluids, with low-cost fabrication, user-friendliness, portability and telemedicine compatibility. In this work, we present expressions of the spontaneous capillary flow velocity in different geometrical configurations. It is shown that relatively large velocities - at the scale of microsystems — can be reached by capillary microflows. Consequently transport distances can be important. *Copyright © 2014 IFSA Publishing, S. L.*

Keywords: Spontaneous capillary flow (SCF), Capillarics, Capillary force, Microgroove, Suspended channels.

1. Introduction

In biotechnology and medicine, point of care (POC) and home care systems are progressively gaining momentum. Such systems must be easily portable, user friendly, robust and low-cost. These systems considerably improve the comfort of patients and the rapidity of the diagnostics [1].

The conventional microfluidic systems use fluids moved by pumps, syringes or electric means, and are not the best solutions when portability and low-cost are an issue. Such systems are bulky and/or require costly, external appliances.

On the other hand, capillary-based systems fulfill the requirements for POC and home-care [2-5]. In these systems, fluids are moved by capillary and surface tension forces. The self-motion of the fluid is called spontaneous capillary flow (SCF). In fact in such systems, the energy source for the fluid motion is the capillary force exerted by the triple line at the front end of the flow. This contrasts with pump or syringe-driven flows where the motor of the motion is a pump or a syringe placed at the back end of the flow.

Moreover, the energy source for capillary-based systems is “packed in” under the form of an adequate surface energy of the walls, while the energy source is external to the biochip when dealing with active systems using pumps, syringes or other electrical means.

Much different geometry of capillary channels exist (Fig. 1). Capillary systems can be confined, i.e. use closed microchannels [6], or they can have an open-surface and the microchannel has the shape of a groove etched in a solid substrate [7-11] or they can even be “suspended”, i.e. the liquids flow between vertical walls without supporting walls at the bottom [12-14].

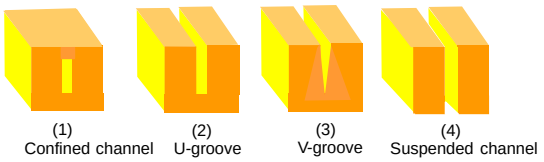

Fig. 1. Different morphologies of capillary channels: (1) rectangular, confined; (2) U-groove; (3) V-groove; (4) rectangular suspended.

For the applications in medicine and biotechnology, it is of utmost importance to determine the sample liquid velocities in such capillary systems. Especially it is essential to know if sufficiently high velocities can be reached in these channels. It is also of importance to know if a system can be totally filled by the sample liquid in an adequate time lapse.

In this work, we derive differential equations for the velocity in capillary channels that collapse in closed form expressions when inertia can be neglected — which is frequent at the microscale. Four geometries are investigated and compared:

1) Rectangular, confined channels;
2) Rectangular, open-surface U-grooves;
3) Triangular, open surface V-grooves;
4) Rectangular, suspended channels (Fig. 1).

The case of the triangular V-groove will not be studied in details; we just report the results of Rye and colleagues [7-9].

It is shown that the velocities are functions of the inverse of the square root of time, and that they are the product of the square root of a "physical" velocity and of a "geometrical" velocity. Depending on the morphology of the channel, relatively large velocities can be obtained, at least in the first few millimeters of the channel.

2. The Dynamics of SCF

We place ourselves in the simplified case where the liquid boundaries are a solid wall with a Young contact angle θ, and — in the case of open channels — a free boundary with air. From a dynamic standpoint, the average velocity of the open microflow can be determined using a balance between capillary forces, surface tension forces and friction with walls [15-18].

The capillary force writes [19, 20]

$$F_{cap} = p_W \gamma \cos\theta - p_F \gamma \,, \tag{1}$$

where γ is the surface tension between the liquid and air, p_W and p_F are the wetted and free perimeters respectively in a cross-section of the channel, as shown in Fig. 2.

On the other hand, the friction force is

$$F_{drag} = \tau S = \tau\, p_W\, z(t)\,, \tag{2}$$

where τ is the wall friction, S is the wetted surface and z is the distance of the interface from inlet which depends on the time t.

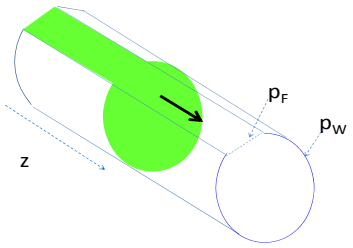

Fig. 2. Sketch of a capillary flow, with the free and wetted perimeters.

On the other hand, the friction force is

$$F_{drag} = \tau S = \tau\, p_W\, z(t)\,, \tag{2}$$

where τ is the wall friction, S is the wetted surface and z is the distance of the interface from inlet which depends on the time t.

The force balance on the fluid flow is then

$$m\frac{dV}{dt} = F_{cap} - F_{drag}\,, \tag{3}$$

where m is the mass of the fluid in the channel and V is the average velocity. The mass of fluid being proportional to the penetration distance, (3) can be written under the form

$$\rho\, z(t) S_c \frac{dV}{dt} = p_W\, \gamma \cos\theta - p_F\, \gamma - \tau\, p_W\, z(t)\,, \tag{4}$$

where S_c is the cross-section area and ρ is the volumic mass of the fluid. The Reynolds number of the fluid being small, the flow is highly laminar and the flow profile is "Poiseuille-like" in the channel. The friction τ then depends on the geometry of the channel and on the average velocity V. Locally, the wall fiction is

$$\tau = \mu\frac{\partial V}{\partial y} = \frac{\mu\, V}{\lambda}\,, \tag{5}$$

where λ is the typical length that depends on the geometry. Upon substitution of (5) in (4), and using the relation $V = dz/dt$, one obtains the second order differential equation for the motion

$$\rho\, S_c \frac{d^2 z}{dt^2} + \frac{\mu}{\lambda}\, p_W \frac{dz}{dt} - \frac{p_W\, \gamma \cos\theta - p_F\, \gamma}{z} = 0 \tag{6}$$

Usually, at the microscale, inertia can be neglected, because the Reynolds number of the order or less than 1. In such a case, relation (6) can be simplified to

$$\frac{dz^2}{dt} = \frac{2\lambda}{\mu}\frac{(p_W\,\gamma\cos\theta - p_F\,\gamma)}{p_W} \tag{7}$$

Integration of (7) yields

$$z = \sqrt{\frac{2\lambda}{\mu}\frac{(p_W\,\gamma\cos\theta - p_F\,\gamma)}{p_W}}\sqrt{t} \tag{8}$$

Finally the capillary velocity is simply the time derivative of z

$$V = \sqrt{\frac{\lambda}{2\mu}\frac{(p_W\,\gamma\cos\theta - p_F\,\gamma)}{p_W}}\sqrt{\frac{1}{t}} \tag{9}$$

Relations (8) and (9) are in agreement with the Lucas-Washburn-Rideal law for the capillary flow inside cylindrical channels [15-17]. Finally the relation between the capillary velocity and the distance is

$$V = \frac{\gamma}{\mu}\frac{\lambda}{z}\left(\cos\theta - \frac{p_F}{p_W}\right) \tag{10}$$

In (8), (9) and (10), the only difficulty is the determination of the friction length λ. In the following, we show on some examples how λ can be approximately calculated.

2.1. Confined Rectangular Channels

In such channels, of width w and height h, the friction can approximately be expressed as

$$F_{drag} \approx 6\mu\frac{V}{w}z(t)\,(2h) + 6\mu\frac{V}{h}z(t)\,(2w) = 12\mu V\,z(t)\left(\frac{w}{h}+\frac{h}{w}\right), \tag{11}$$

where μ is the dynamic viscosity of the fluid. The friction length is then

$$\lambda = \frac{1}{6}\frac{w+h}{\left(\frac{w}{h}+\frac{h}{w}\right)} \tag{12}$$

On the other hand, the capillary force is

$$F_{cap} = 2\,\gamma\cos\theta\,(w+h) \tag{13}$$

The travel distance as a function of the time is then given by

$$z = \sqrt{\frac{\gamma\cos\theta(w+h)}{3\mu\left(\frac{w}{h}+\frac{h}{w}\right)}}\sqrt{t} \tag{14}$$

Note that, because the channel is closed, w and h are reversible in relation (14). If we note e the channel aspect ratio $e=w/h$, the capillary velocity is given by

$$V = \sqrt{\frac{\gamma\cos\theta(w+h)}{12\mu\left(\frac{w}{h}+\frac{h}{w}\right)}}\sqrt{\frac{1}{t}} = \sqrt{\frac{\gamma}{\mu}\frac{h}{t}\frac{e\cos\theta(1+e)}{12\left(1+e^2\right)}} = \sqrt{\frac{\gamma}{\mu}\frac{h}{t}}\sqrt{f_1}, \tag{15}$$

where

$$f_1 = \frac{e\cos\theta(1+e)}{12\left(1+e^2\right)} = \frac{\lambda}{2h}\cos\theta \tag{16}$$

is the non-dimensional function that depends on the geometry (and on the contact angle θ). Relation (15) states that the velocity is the product of the square root of a "physical velocity" $\sqrt{\gamma/\mu}$ — which depends on the properties of the fluid—by the square root of a "geometrical velocity" $\sqrt{h/t}$ and by a characteristic non-dimensional function $\sqrt{f_1}$. Finally, eliminating the time from (14) and (15) produces the relation between the velocity and the penetration distance

$$V = 2\frac{\gamma}{\mu}\frac{h}{z}f_1 \tag{17}$$

2.2. Open Rectangular U-grooves

The SCF in open rectangular U-grooves is shown in Fig. 3.

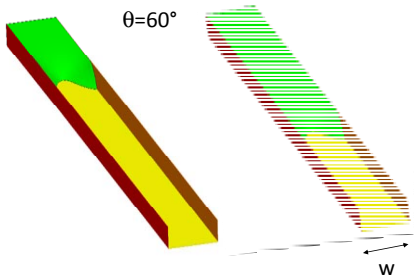

Fig. 3. SCF in a U-groove (quasi-static Evolver calculation).

Following the same approach as that of preceding section, the friction length is given by

$$\lambda = \frac{1}{6}\frac{w+2h}{\left(\frac{w}{h}+\frac{2h}{w}\right)} \tag{18}$$

and

$$z = \sqrt{\frac{\gamma}{\mu}}\sqrt{ht}\sqrt{\frac{[\cos\theta(e+2)-e]}{3\left(\frac{2}{e}+e\right)}} \quad (19)$$

The capillary velocity is then

$$V = \sqrt{\frac{\gamma}{\mu}\frac{h}{t}\frac{[(e+2)\cos\theta - e]}{12\left(\frac{2}{e}+e\right)}} = \sqrt{\frac{\gamma}{\mu}}\sqrt{\frac{h}{t}}\sqrt{f_2} \quad (20)$$

relation which has the same form as (15) with a different geometrical function f_2:

$$f_2 = \frac{[(e+2)\cos\theta - e]}{12\left(\frac{2}{e}+e\right)} \quad (21)$$

The penetration as a function of the distance z is then

$$V = 2\frac{\gamma}{\mu}\frac{h}{z}f_2 \quad (22)$$

2.3. Suspended Rectangular Channels

A suspended microflow is a flow that uses capillary forces and surface tension to fill and maintain a fluid in microscale structures devoid of a ceiling and floor (Fig. 4A). These flows have the advantage to be accessible on both sides, from above and from below.

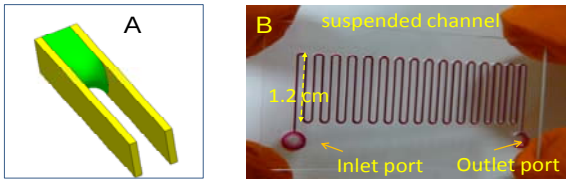

Fig. 4. A: sketch of a suspended flow;
B: SCF in a suspended channel (w=300 µm, h= 1 mm).

The dynamics of this kind of microflow is derived in the same manner as for U-grooves [14], and we find

$$\lambda = \frac{w}{6} \quad (23)$$

$$z = \sqrt{\frac{\gamma}{\mu}ht}\sqrt{\frac{[e(\cos\theta - e)]}{3}} \quad (24)$$

and

$$V = \sqrt{\frac{\gamma}{\mu}\frac{h}{t}}\sqrt{\frac{[e(\cos\theta - e)]}{12}} = \sqrt{\frac{\gamma}{\mu}\frac{h}{t}}\sqrt{f_3}, \quad (25)$$

where

$$f_3 = \frac{[e(\cos\theta - e)]}{12} \quad (26)$$

and

$$V = 2\frac{\gamma}{\mu}\frac{h}{z}f_3 \quad (27)$$

3. Experiments

In this section, we experimentally checked the results of the preceding section.

Clearly the Formulas (8) and (9) collapse to the Lucas-Washburn-Rideal equation in the case of the cylinder: in such a case λ=R/4, where R is the radius of the cylinder.

Let us consider first the results obtained by Han and coworkers [21] for confined nanochannels of approximately rectangular cross section, and coated by a SiO_2 layer. The nanochannels are 900 nm wide and 50 nm deep. Four different liquids were used: water, a 40 % ethanol solution, pure ethanol and isopropanol. Relation (14) is compared to the experimental results in Fig. 5. A good agreement is observed using the same physical properties of the liquids indicated in the publication. Note that the Washburn kinetics is respected, i.e. the travel distance is proportional to the square root of time. Note also that the contact angle is constant because the plots are linear: the capillary number being small, the advancing contact angle is constant and equal to the static contact angle.

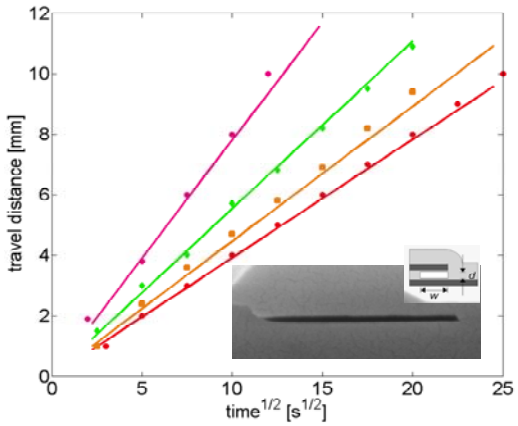

Fig. 5. Travel distances vs. square root of time in a silicon nanochannel coated by a silica layer (w=900 nm, h=50 nm).

Second, experiments using rectangular U-groove have been performed: the channel is shown in insert of Fig. 6. The device is made of PMMA and hydrophilically treated with plasma O_2. Again the agreement between experiments and relation (19) is satisfactory.

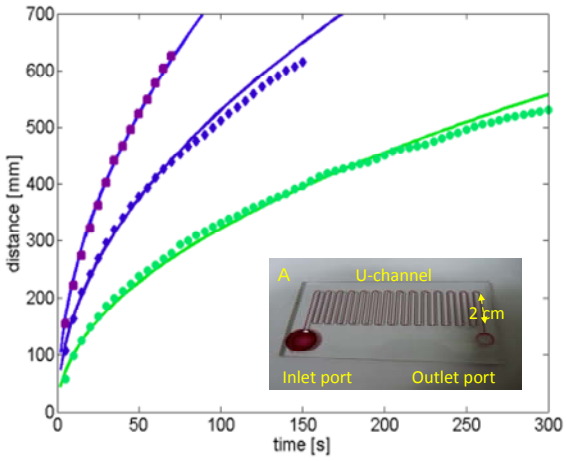

Fig. 6. SCF in a winding, rectangular, U-groove channel etched in PMMA (w=300 μm, h=1 mm) for three aqueous liquids. The three liquids are water dyed with different food coloring at different concentration. Dots are experimental results while continuous lines correspond to relation (19).

Finally, experiments using a suspended channel have been conducted: the channel is shown in Fig. 4B and in insert of Fig. 7. The device is made of PMMA and hydrophilically treated with plasma O_2.

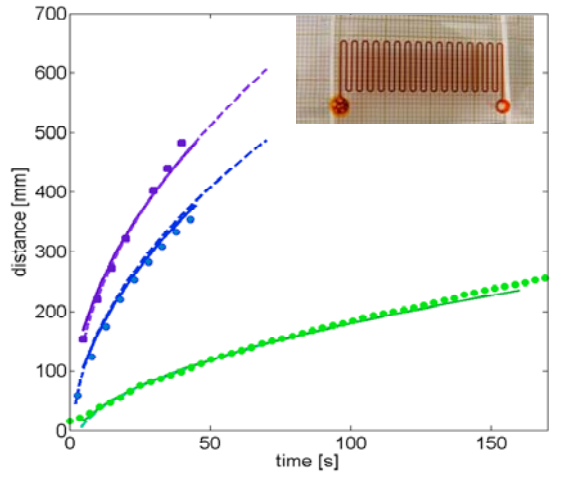

Fig. 7. Penetration distance as a function of time for three aqueous liquids. The aqueous liquids are water dyed with different food coloring at different concentration. Dots correspond to the experimental results, the continuous lines to the theoretical solution without inertial terms — relation (24), and dotted lines to the theoretical solution with the inertial terms — relation (6).

4. Comparisons

When comparing the different geometrical configurations, it is the geometrical function f that produces the velocity difference (Fig. 8). Fig. 9 shows the penetration distance in the channel as a function of the elapsed time for two different aspect ratios e=0.22 and e=0.63 and a contact angle of 30°. We have added the case of the open triangular channel described by Rye and colleagues [15-17], where the dynamics is calculated by the Lucas-Washburn-Rideal expression with an equivalent hydraulic radius. The liquid is water, with a surface tension γ= 72 mN/m, and a dynamic viscosity μ=0.001 Pa.s.

The closed, open-U and suspended channels stay always in the same order for the velocity magnitude: the velocity is largest for the confined channel, then for the U-groove, and then for the suspended channel. On the other hand, the velocity in the V-groove varies considerably with the groove angle. Note that the aspect ratio e in the case of the V-groove is related to the groove angle by the relation $\tan(\alpha/2) = w/2h = e/2$. For e=0.22, α~6°, and for e=0.63, α~35°.

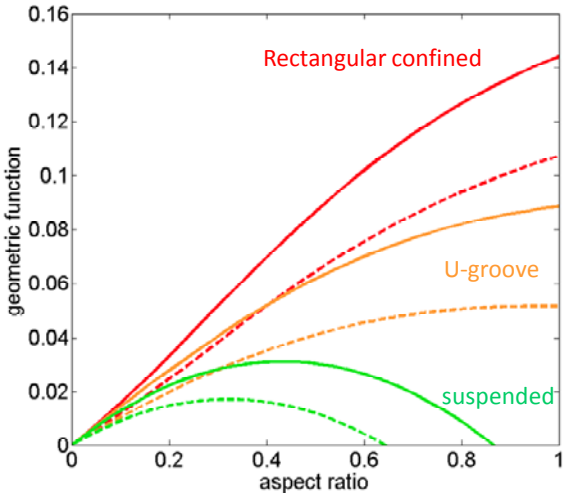

Fig. 8. Comparison of the penetration distance with the aspect ratio for confined-rectangular, open-rectangular and suspended channels. Continuous and dotted lines correspond respectively to a contact angle of 30° and 50°.

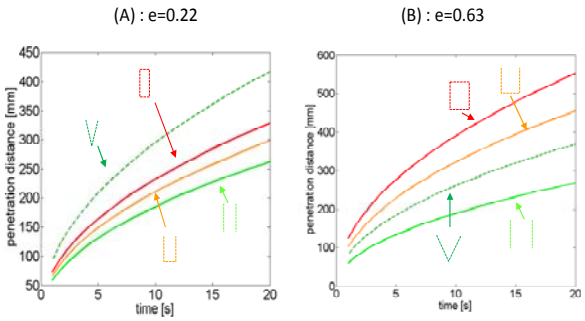

Fig. 9. Comparison of the penetration distance between the different geometries. A: aspect ratio e=0.22. B: aspect ratio e=0.63. In both cases the contact angle is 30°.

5. Conclusions

In this work, the capillary velocities in closed channels, U-grooves and suspended channels have been investigated. Closed form expressions for the

velocities with a dependency as $\sqrt{1/t}$ have been found, in agreement with the Lucas-Washburn-Rideal approach.

Relations between travel distance and time, and capillary velocity and time have been derived for different channel geometries, and they show the same canonical form. They only differ by a non-dimensional "form" function typical of each channel.

These expressions can be extrapolated to composite walls of different materials [14] — which is often the case with closed channels where the cover can be made of a different material.

It seems that there is a need to investigate further the velocity in very narrow V-grooves since the usual expression of the literature diverges when the groove angle decreases towards zero. Moreover, the non-Newtonian aspect is still to be investigated since biological fluids have often a shear-thinning behavior, and their viscosity increases with the decrease of the velocity in the capillary channel.

References

[1]. G. J. Kost, Principles and Practice of Point-of-Care Testing, *Lippincott Williams & Wilkins*, June 2002.

[2]. P. Yager, T. Edwards, E. Fu, K. Helton, K. Nelson, M. R. Tam, B. H. Weigl, Microfluidic diagnostic technologies for global public health, *Nature*, Vol. 442, Issue 7101, 2006, pp. 412-418.

[3]. A. W. Martinez, S. T. Phillips, G. M. Whitesides, Diagnostics for the developing world: microfluidic paper-based analytical devices, *Anal. Chem.*, Vol. 82, 2010, pp. 3–10.

[4]. L. Gervais, N. de Rooij, E. Delamarche, Microfluidic chips for point-of-care immunodiagnostics, *Adv. Mater.*, Vol. 23, Issue 24, 2011, pp. H151–H176.

[5]. L. Gervais, E. Delamarche, Toward one-step point-of-care immunodiagnostics using capillary-driven microfluidics and PDMS substrates, *Lab Chip*, Vol. 9, 2009, pp. 3330-3337.

[6]. R. Safavieh, D. Juncker, Capillarics: pre-programmed, self-powered microfluidic circuits built from capillary elements, *Lab Chip*, Vol. 13, 2013, pp. 4180-4189.

[7]. R. R. Rye, F. G. Yost, Wetting Kinetics in Surface Capillary Grooves, *Langmuir*, Vol. 12, 1996, pp. 4625-2627.

[8]. F. G. Yost, R. R. Rye, J. A. Mann, Solder wetting kinetics in narrow V-grooves, *Acta Materialia*, Vol. 45, 1997, pp. 5337-5345.

[9]. L. A. Romero, F. G. Yost, Flow in an open channel capillary, *Journal of Fluid Mechanics*, Vol. 322, 1996, pp. 109-129.

[10]. J. Berthier, K. Brakke, E. P. Furlani, I. H. Karampelas, G. Delapierre, Open-Surface Microfluidics, in *Proceedings of the Nanotech Conference*, Washington DC, 15-19 June 2014.

[11]. J. Berthier, N. Villard, A.-G. Bourdat, G. Nonglaton, C. Pudda, F. Boizot, G. Costa, C. Fontelaye, G. Delapierre, On the velocity of spontaneous capillary flows in confined and open microchannels, in *Proceedings of the Nanotech Conference*, Washington DC, 15-19 June 2014.

[12]. J. Berthier, K. Brakke, The Physics of Microdroplets, *Scrivener-Wiley Publishing*, May 2012.

[13]. B. P. Casavant, E. Berthier, A. B. Theberge, J. Berthier, S. I. Montanez-Sauri, L. L. Bischel, K. Brakke, C. J. Hedman, W. Bushman, N. P. Keller, D. J. Beebe, Suspended microfluidics, *PNAS*, Vol. 110, Issue 25, 2013, pp. 10111-10116.

[14]. J. Berthier, K. A. Brakke, D. Gosselin, A.-G. Bourdat, G. Nonglaton, N. Villard, G. Laffite, F. Boizot, G. Costa, G. Delapierre, Suspended microflows between vertical parallel walls, *Microfluid. Nanofluid.*, September 2014.

[15]. R. Lucas, Ueber das Zeitgesetz des Kapillaren Aufstiegs von Flussigkeiten, *Kolloid Z*, Vol. 23, 1918, pp. 15-22.

[16]. E. W. Washburn, The dynamics of capillary flow, *Phys. Rev.*, Vol. 17, 1921, pp. 273-283.

[17]. E. K. Rideal, On the flow of liquids under capillary pressure, *Philos. Mag. Ser.*, Vol. 6, Issue 44, 1922, pp. 1152-1159.

[18]. J. Berthier, K. A. Brakke, E. P. Furlani, I. H. Karampelas, V. Poher, D. Gosselin, M. Cubizolles, P. Pouteau, Whole blood spontaneous capillary flow in narrow V-groove microchannels, *Sensors and Actuators B*, 206, January 2015, pp. 258–267.

[19]. J. Berthier, K. Brakke, E. Berthier, A general condition for spontaneous capillary flow in uniform cross-section microchannels, *Microfluid. Nanofluid. Journal*, Vol. 16, 2014, pp. 779-785.

[20]. F. F. Ouali, G. McHale, H. Javed, C. Trabi, N. J. Shirtcliffe, M. I. Newton, Wetting considerations in capillary rise and imbibition in closed square tubes and open rectangular cross-section channels, *Microfluid. Nanofluid.*, Vol. 15, 2013, pp. 309-326.

[21]. A. Han, G. Mondin, N. G. Hegelbach, N. F. de Rooij, U. Staufer, Filling kinetics of liquids in nanochannels as narrow as 27 nm by capillary force, *Journal of Colloid and Interface Science*, Vol. 293, 2006, pp. 151-157.